NUMERICAL SIMULATION OF SPIRAL-STRAND CABLES SUBJECTED TO HIGH VELOCITY FRAGMENT IMPACT

***R. Judge[1,2], Z. Yang[1], S.W. Jones[1] & G. Beattie[2]**

[1]School of Engineering, the University of Liverpool, L69 3GH
[2]Arup, L3 9QJ

*ryan.judge@liv.ac.uk/ryan.judge@arup.com

Key Words: *penetration; high-velocity impact; fragment; structural cables; Johnson-Cook model*

ABSTRACT

This paper presents the results of a numerical study carried out to evaluate the response of high-strength steel spiral-strand cables, when subjected to high velocity fragment impact. A detailed numerical model of a 60 mm diameter spiral-strand cable subjected to impact from a 20 mm fragment simulating projectile has been developed for analysis in LS-DYNA. Detailed consideration was given to the complex geometry of the cable, wire-to-wire contact and friction, cable-end boundary conditions and appropriate material modelling. Fragment velocities between 200 and 1400 m/s were modelled to assess the penetration and perforation resistance of the cable and to study the magnitude of localised cross-sectional cable damage. The numerical results were validated against initial laboratory tests. In both the tests and numerical simulations none of the cables were perforated by the fragments and good agreement was seen in the damage area, the fragment penetration depth and the wire splay phenomenon.

1. Introduction

Spiral-strand cables are widely used in the design and construction of sports stadia and bridges as depicted in Fig. 1, but their robustness and resilience against explosively formed fragment impact, whether accidental or malicious, remains largely unknown. Very little research has been carried out to study the effects such an impact has on the cables, cable terminations and the surrounding structure. Zoli [1] assessed the vulnerability of the typical cable types used on cable-stayed/suspended bridges. It was highlighted that there are a number of potential mechanisms capable of inducing abrupt cable loss including the impact of explosively formed fragments travelling at high velocity.

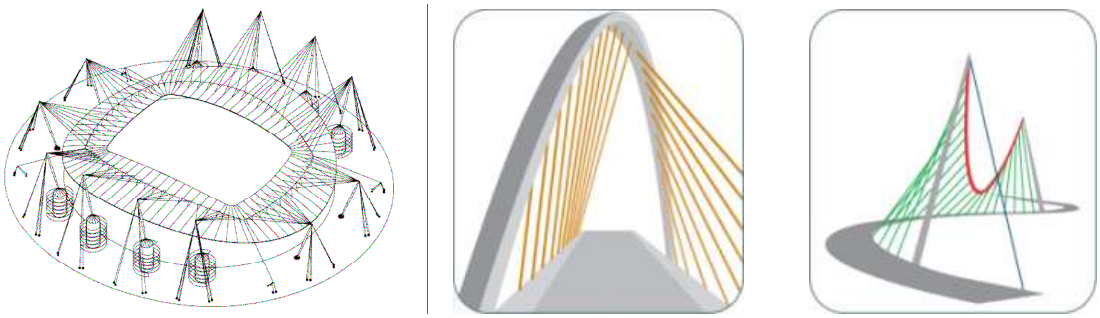

Fig.1 Use of cables in stadia and bridges

In this paper a detailed numerical model of a 60 mm diameter spiral-strand cable subjected to impact from a 20 mm fragment simulating projectile (FSP) has been developed for analysis in LS-DYNA [2]. The FSP was used in the absence of real fragment data from the types of explosion mentioned above and for the purpose of experimental validation. Detailed consideration was given to the complex geometry of the cable, wire-to-wire contact and friction, cable-end boundary conditions and appropriate material modelling. Key material parameters were derived for the modified Johnson-Cook (MJC) constitutive relation [3] and the Cockcroft-Latham (CL) fracture criterion [4], both of which were used to model the material of the cable and the FSP. Fragment velocities between 200 and 1400 m/s were considered to evaluate the penetration and perforation resistance of the cable and to study the magnitude of localised cross-sectional cable damage. Initial laboratory tests were carried out to validate the numerical simulations. In these experiments, six un-tensional 60-mm diameter spiral-strand cables were tested by firing standard 20-mm FSPs at the cables using a high powered powder gun.

2. Laboratory tests of cables

Spiral-strand cables are comprised of many individual high strength round steel wires. The wires are manufactured from high carbon steel and have nominal tensile strengths in the range of 1550 to 1770 MPa. The cables are manufactured using circumferential layers spirally wound around a central straight wire and spun in opposite directions to minimise the residual torque and de-coiling as a result of the elastic-stresses induced in the wires during the spinning process. A typical schematic of a spiral-strand cable is shown in Fig. 2.

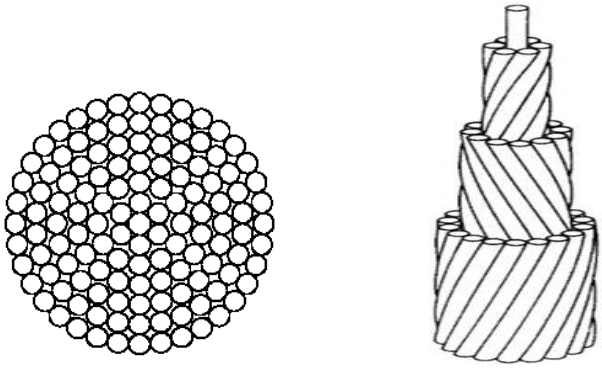

Fig.2 Cross-section and side elevation of a typical spiral-strand cable

The cable tested and modelled in this study is a 60-mm diameter un-tensioned spiral-strand cable. The cable consists of one central wire and seven outer layers and is manufactured from 120 wires in total. The diameter of the wires ranges from 3.2 to 5.8 mm, and their nominal tensile strength is 1770 MPa.

Six 1-m length cables were provided by Bridon International Ltd, one of the leading rope and cable manufacturers in Europe, and tested at Shrivenham Defence Academy in the UK. Each cable was mechanically fitted with a 'wrap-around' steel coil at both ends to mimic the end conditions when they are socketed into steel terminations. The cables were clamped to a simple test frame as shown in Fig. 3. A high powered powder gun was used to fire the standard 20-mm FSP. The fragment velocities 1328 m/s, 680 m/s, 580 m/s, 501 m/s, 360 m/s and 297 m/s were tested. The initial and residual fragment velocities were measured by an optical velocity measurement system. A high speed video camera was used to capture the fragment impact events.

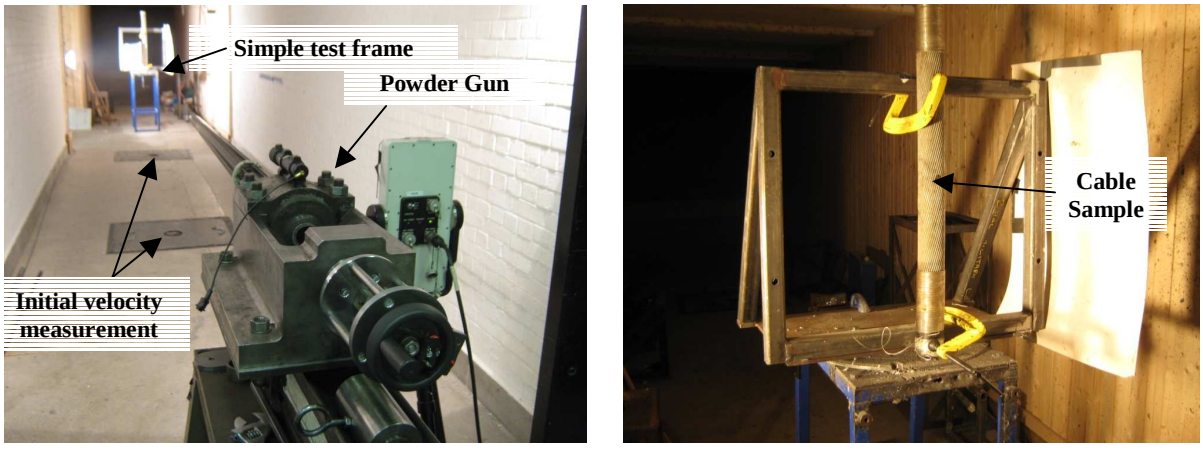

Fig.3 Experimental set-up for cables under impact

3. Numerical Model

The numerical model of the cable was constructed using a staged process illustrated in Fig. 4 and briefly discussed here. Firstly, a central wire made up of 8-noded single integration point solid elements was made. Then each subsequent layer was constructed in the same manner using cross-sectional wire co-

ordinates until all wires were positioned parallel to one another in approximate locations. This was carried out using LS-PrePost [5]. The model consisting purely of nodes and elements was then transferred into Oasys PRIMER [6] and a JavaScript was then imported to morph the geometry of each layer around the central wire to create the spiralling based on the lay lengths and lay angles provided by Bridon. For reference, the lay length describes the length after which a wire reappears at the same angular position along the longitudinal axis of the cable; hence the lay length is different for each individual layer. The script can also be used to construct spiral strands of any diameter given the lay lengths and lay angles are provided.

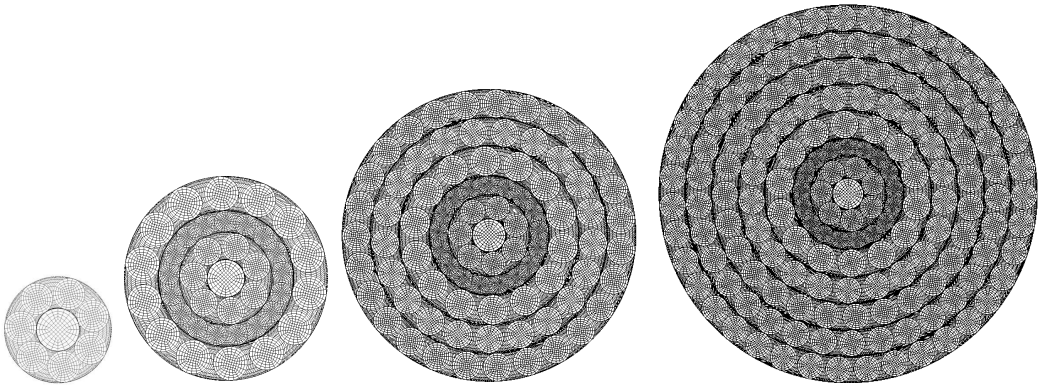

Fig.4 Construction sequence of the finite element model of a 60 mm diameter spiral-strand cable

In the absence of data on fragments generated from accidental or malicious explosions, the fragment was modelled as a standard 20-mm FSP as shown in Fig. 5a and b. The FSP's are typically used in ballistics testing. They are based on and characterised by the break-up of artillery shells when detonated. On detonation, the fragmentation pattern is relatively random and not suitable for repeatable laboratory testing. The same is assumed for fragments generated from accidental or malicious explosions. In order to provide a repeatable simulation of a fragment generated from an explosion the FSP is used as standard. The fragment has been simplified in the numerical model to a 20 mm diameter x 20 mm long cylinder also made of 8-noded solid elements with single integration point as shown in Fig. 5c.

(a) (b) (c)

Fig.5 Fragment simulating projectile and the finite element representation

In the simulations, initial velocities similar to those used in the tests were assigned to the FSP under the *INITIAL_VELOCITY card. To limit the computational cost, a cable segment of 250 mm long was modelled. This was reasonable because the cable global behaviour would be secondary to the local behaviour at such high impact velocities [7]. Studies are ongoing to investigate the effects of the cable length on the impact, penetration and perforation resistance of the cables especially at the lower fragment velocity range. The full numerical model consisting of the cable and fragment is shown in Fig 6. The colour in the wires represents individual *PART references for each wire. There are 10,692,999 elements and 10,762,427 nodes in total. Each simulation took approximately 12 hours for a typical explicit simulation to complete on a Dell Precision 64-bit T5400 workstation with 4 CPUs and 32GB RAM.

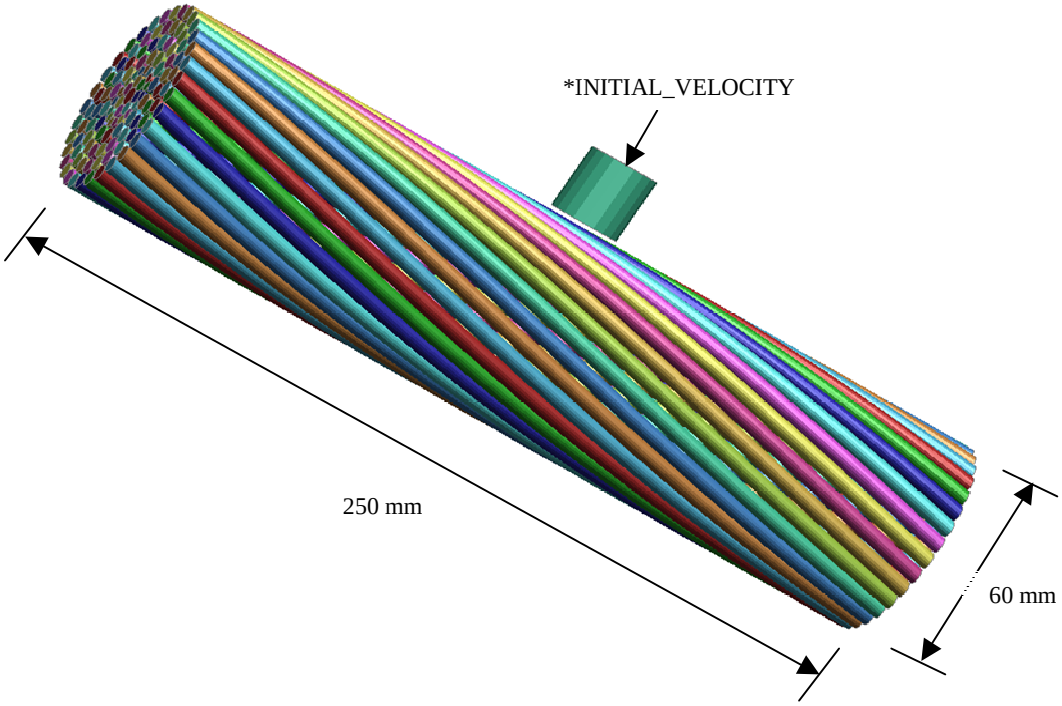

Fig.6 Complete finite element model with cable and fragment

Contact between adjacent wires and between the wires and the fragment was modelled using a *ERODING_SINGLE_SURFACE penalty formulation in LS-DYNA, which can not only model the wire to wire contact, but regenerate contact surfaces when fully damaged elements are removed from the mesh. A global dynamic friction coefficient of 0.2 was used in all simulations for modelling wire-to-wire and fragment-to-wire friction. The Flanagan-Belytschko stiffness based hourglass control was also applied to all elements using the *HOURGLASS card.

Two boundary conditions at the cable ends were considered using the *BOUNDARY_SPC cards. The first condition allowed for only axial translational of the wires at both ends of the cable, while the second constrained all 6 degrees of freedom to zero. The first condition was considered to be representative of the test conditions as discussed later, and the second was considered to be closer to the real end conditions of

a cable in a cable supported structure. It is viewed that the end constraint lies somewhere between both boundary conditions when account is made for wire-to-wire and wire-to-coil frictional resistance.

4. Material constitutive models

A complete material description under impact involves not only the stress-strain response highly dependent on strain, strain-rate, temperature and loading history, but also accumulation of damage and failure [7]. A slightly modified version of the Johnson-Cook constitutive relation [3] has been used in this study for both the cable and fragment materials. The model is typically denoted as the MJC model in the literature to distinguish it from the original model [8]. The equivalent stress is expressed as

$$\sigma_{eq} = [A + B\varepsilon_{eq}^{\ n}][1 + \acute{\varepsilon}_{eq}^{*}]^{C}[1 - T^{*m}] \tag{1}$$

where A is the yield strength, B the hardening modulus, ε_{eq} the equivalent plastic strain, n the hardening coefficient, C is the strain rate sensitivity coefficient, and $\acute{\varepsilon}_{eq}^{*}$ a dimensionless plastic strain rate equal to $\acute{\varepsilon}_{eq} / \acute{\varepsilon}_0$ where $\acute{\varepsilon}_0$ is a user defined strain rate . The temperature dependence is given by the homologous temperature T^*

$$T^* = (T - T_r)/(T_m - T_r) \tag{2}$$

where T is the absolute temperature, T_r the room temperature, T_m the melting temperature and m the thermal softening coefficient. In Eq. (1), the terms in the three brackets represent the strain hardening, the strain-rate sensitivity and the temperature softening, respectively.

The temperature increment due to adiabatic heating is calculated by

$$\Delta T = \int_0^{\varepsilon_{eq}} \chi \frac{\sigma_{eq} d\varepsilon_{eq}}{\rho C_P} \tag{3}$$

where ρ is the material density, C_p the specific heat and χ the Taylor-Quinney coefficient that represents the proportion of plastic work converted into heat.

Material failure in both the cable and fragment was modelled using the Cockcroft-Latham (CL) fracture criterion [4] which assumes that fracture occurs when the plastic work W per unit volume exceeds a critical value W_{cr}:

$$W = \int_0^{\varepsilon_{eq}} \langle \sigma_1 \rangle d\varepsilon_{eq} \leq W_{cr} \tag{4}$$

where σ_1 is the maximum principal stress, $\langle \sigma_1 \rangle = \sigma_1$ when $\sigma_1 \geq 0$ and $\langle \sigma_1 \rangle = 0$ when $\sigma_1 < 0$. The critical

value of W_{cr} is the area under the true stress-strain curve and can be determined from simple uniaxial tensile tests. To initiate element failure during impact, the model is coupled with an algorithm that erodes damaged elements when *W* reaches *Wcr*. In addition to Eq. (4), a temperature based erosion criteria was also adopted to remove elements when their temperature reaches $T_c^*=0.9T_m$, because at such high temperatures, the material is too soft to resist impact [9]. Both the MJC constitutive relation and the CL fracture criterion are available under *MAT_107 (*MODIFIED JOHNSON COOK MODEL) [2]. The MJC and CL parameters for the wires are tabulated in Table 1. These are based on Brigman corrected true stress-strain data derived by Walton in [10] for the 1770 MPa strength wire.

Table 1 Material properties for MJC and CL parameters used for steel wires

Strain Hardening	Strain rate Hardening	Temperature Softening	CL Failure	Temperature cut-off
A = 1670 (MPa) B = 375 (MPa) n = 0.81	$\dot{\varepsilon}_0$ = 5 x 10^{-4} (s^{-1}) C = 0.0010	T_r = 293 (K), T_m = 1775 (K), m = 1.0	ε_f = 0.635 W_{cr} = 1350 (MPa)	T_c^* = 1598 (K)

The FSP is typically manufactured from 4340 steel. Therefore the MJC and CL material parameters have been taken directly from [8] and listed in Table 2.

Table 2 Material properties for MJC and CL parameters used for FSP

Strain Hardening	Strain rate Hardening	Temperature Softening	CL Failure	Temperature cut-off
A = 792 (MPa) B = 510 (MPa) n = 0.26	$\dot{\varepsilon}_0$ = 5 x 10^{-4} (s^{-1}) C = 0.014	T_r = 293 (K), T_m = 1775 (K), m = 1.0	ε_f = 1.0 W_{cr} = 1350 (MPa)	T_c^* = 1598 (K)

Other material parameters used in the simulations for both the cable and fragment are listed in Table 3.

Table 3 Common material properties

E = 210,000 (MPa),	υ = 0.3,	ρ = 7850 kg/m^3,	C_p = 452 J/kgK,	χ = 0.9

5. Results and discussion

5.1 Laboratory tests

Fig. 7 shows the damaged cables in the laboratory tests for three velocities, 1328 m/s, 680 m/s and 297 m/s.

(a) (b) (c)

Fig.7 Damaged cables in the laboratory tests from fragment velocities (a) 1328 m/s (b) 680 m/s and (c) 297 m/s

In all the tests the fragments did not perforate the cables and significant penetration was only observed for the 1328 m/s and 680 m/s fragment velocities. The damage sustained was localised to the impact zone, which was small relative to the cable length. Post-test inspections found that a number of wires at the end of the cable had been pulled through the steel coil, especially for the 1328 m/s fragment velocity. As a result, significant wire-splay (horizontal wire translation) at the impact zone was observed as can be seen in Fig. 7a.

Significant wire flattening was observed in the tests on impact. This appears to be a result of the wires in a specific layer being pressed against the wires below in a lower layer. This leads to tensile failure in a thinned section of a wire.

The measured fragment penetration depth (FPD) was less than half the diameter of the cable in all cases. As expected, a significant decrease in the FPD was observed as the velocity and thus kinetic energy of the fragment was reduced (see Fig. 10).

5.2 Numerical simulations

Fig. 8 shows the cables with damage fringes obtained from the numerical simulations using the first boundary condition for the 1328 m/s, 680 m/s and 297 m/s fragment velocities. The fringes in Fig. 8 represent regions of high plastic strain. The simulated results from the second boundary condition are shown in Fig. 9.

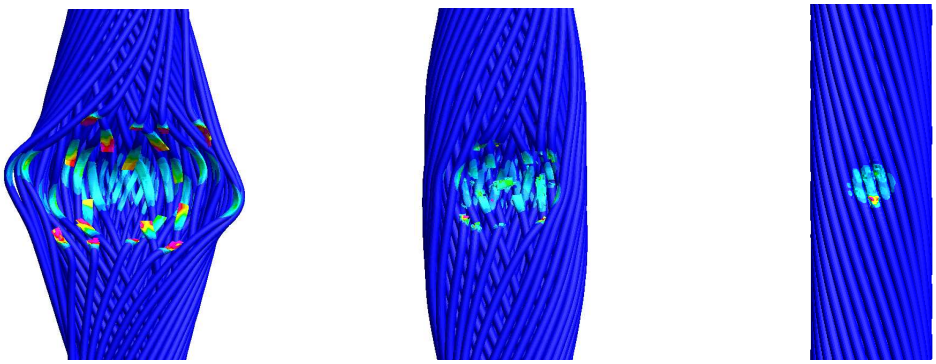

(a) (b) (c)

Fig.8 Predicted cable damage from fragment velocities (a) 1328 m/s (b) 680 m/s and (c) 297 m/s using the first boundary condition.

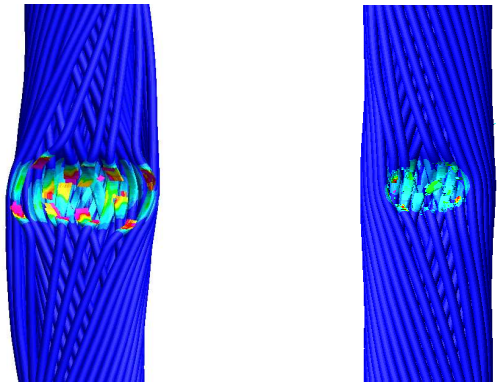

(a) (b)

Fig.9 Predicted cable damage from fragment velocities (a) 1328 m/s (b) 680 m/s using the second boundary condition.

Comparison of Fig. 7 and Figs. 8-9 shows that the first boundary condition led to predictions closer to the test observations than the second, with respect to the FPD, the number of fractured wires, wire flattening and wire-splay phenomenon across all fragment velocities considered. This is because the first allowed axial translation of the wires near the ends of the cable, which was observed in the tests and discussed in section 5.1, whereas the second fully fixed both ends, leading to less dramatic deformation at the impact zone. There was negligible difference in the fragment penetration depth and overall damage magnitude when the second boundary condition was considered. The FPD-fragment velocity curves for all the tests and numerical simulations using the first boundary condition are compared in Fig 10, where good agreement can be seen.

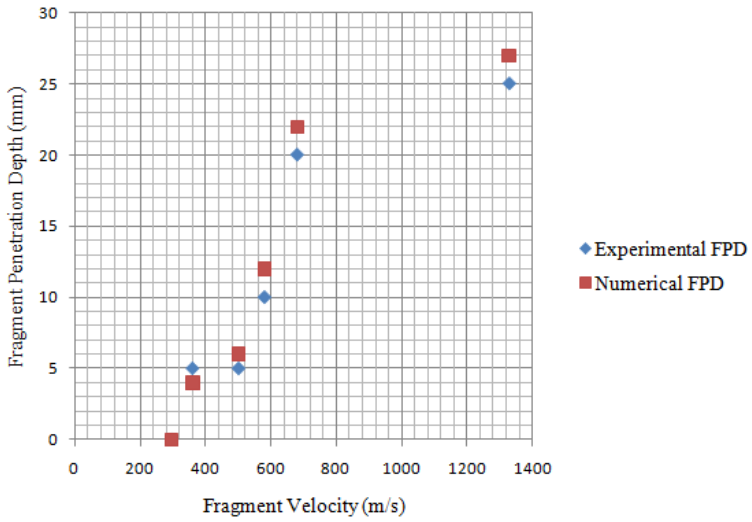

Fig.10 Experimental and numerical fragment penetration depths

6. Conclusions

This study has developed a full 3D finite element model for spiral-strand cables subjected to high velocity fragment impact for analysis in LS-DYNA. The model considers the complex topology of the cable, complicated wire-to-wire contact and friction, and realistic material constitutive laws. A cable with 120 wires was modelled as an example and the numerical results were satisfactorily validated against initial laboratory tests for six fragment velocities, in terms of the global cable response, the localised damage area, and the penetration depth. Further studies are ongoing to investigate the effects of other key factors such as the cable length and cable pre-stress on the impact resistance of the cables. This study represents a first step in gaining a better understanding of the robustness and resilience of structural cables against high velocity fragment impact, using both numerical modelling and experimental validation. The research outcomes will be used to better inform structural designs where physical security is a key requirement.

Acknowledgments

This study is funded by UK EPSRC and ARUP through a CASE Award (No. CASE/CAN/07/107). The cables tested were provided by Bridon International Ltd and the tests were carried out with the help of Prof. Ian Horsfall at Shrivenham Defence Academy, Cranfield University, UK. Their kind contributions to this project are highly appreciated.

References

[1] Zoli, T. Some Considerations in the Design of Long Span Bridges against Progressive Collapse. In: Proceedings of the International Bridge Conference 2009.

[2] LSTC. LS-DYNA users manual. Version 971. Livermore Software Technology Corporation, CA, USA, 2006.

[3] Borvik T, Hopperstad OS, Berstad T and Langseth M. Computational model of visco-plasticity and ductile damage for projectile impact. European Journal of Mechanics and Solids, 20, 685-712, 2001.

[4] Cockcroft MG, and Latham DJ. Ductility and the workability of metals. Journal of the Institute of Metals, 96, 33-9, 1968.

[5] LSTC. LS-PrePost Users Manual. Version 3.0. Livermore Software Technology Corporation, CA, USA, 2009.

[6] Oasys Ltd. PRIMER Users Manual. Version 9.4. Arup, Solihull, UK, 2009.

[7] Zukas JA. High Velocity Impact Dynamics. New York: Wiley, 1990.

[8] Johnson GR, and Cook WH. A constitutive model and data for metals subjected to large strains, high strain rates and high temperatures. In: Proceedings of the Seventh International Symposium on Ballistics, The Hague, 1983

[9] Borvik T, Dey S, and Clausen AH. Perforation resistance of five different high strength steel plates subjected small-arms impact. International Journal of Impact Engineering, 36, 948-964, 2009.

[10] Walton JM. Contact stresses in wire rope. MPhil Thesis, University of Leeds, 1987